

Pattern Recognition and Analysis for Circuit Fabrication by Ink Jet Printing

Ming-Huan Yang, Shawn Chiu, Chung-Wei Wang, Chih-Jian Lin, Jane Chang and Kevin Cheng
OES/Industrial Technology Research Institute, Hsinchu, Taiwan, Republic of China
E-mail: ChaoKaiCheng@itri.org.tw

Abstract. Traditional methods for patterning conductive materials, such as screen-printing and photolithography, are complex and time-consuming. In this paper, we successfully combined three processes: Self-assembly polyelectrolyte (SAP) surface treatment, microdispensing catalyst patterning on the substrate, and electroless plating to form metal circuits. Due to the porous structure, these polyelectrolyte membranes are of great benefit to the absorption of the catalyst used for metal deposition. Hence, the processes above can form excellent metal pattern for various substrates, for example, PET, Glass, PI, FR-4, etc. The result has been verified by IPC 6013 standard for flexible substrate. This study also developed an image analysis method to validate the reliability of this ink jet printed circuit. It included the steps of threshold setting, erosion operation, template calibration, filtering, and edge-enhancement. After image analysis, the line width was of 135 μm on the average and the standard deviation was of 3.5 μm . The maximum blurring rate of the edge of the line observed is within $\pm 15\%$. © 2006 Society for Imaging Science and Technology.

[DOI: 10.2352/J.ImagingSci.Technol.(2006)50:3(251)]

INTRODUCTION

Conventional PCB (printing circuits board) fabrication process comprises the steps of laminating dry metal film to the substrate, spinning photo resist, pattern masking, exposing, developing, etching the photo resist, metal plating, and resist cleaning, etc. For many years, screen printing and photolithography have been the predominant methods of imaging in PCB manufacturing processes. Both methods have their own individual strengths and weaknesses. Manufacturers select the most appropriate process for their requirements in primary tracking image, solder mask application and legend printing.¹ These methods suffer from the drawback of being analogue processes, and hence require conversion from a digital data file to a printable image via production of a screen or photo tool. This adds cost and time delays to the preparation of boards, particularly for prototyping and short-run production.

Ink jet printing as applied to patterning for PCB application offers advantages of low capitalization of equipment, high material efficiency, noncontact processing, and elimination of photolithography process.¹ Some have reported on ink jet printing of metal organic decomposition inks with nano-particle additions or organic metal precursor. Near-bulk conductivity of printed and sprayed metal films has

been achieved for Ag and Ag nanocomposites.^{2,3} A major challenge in applying direct ink jet nano-particle process is the ink formulation. The inks must contain the appropriate precursors and a carrier compound, and may further contain various binders, dispersants, and adhesion promoters, depending on the nature of the precursor and the particular application. Ink composition is critical because it defines the process in which the ink is jetted, the adhesion to the substrate, the line resolution and its profile, and the electronic properties of metal formation.³ Direct ink jet printing of nanoparticle currently faces the obstacles of insufficient adhesion to the substrate, and the need of high temperature process (200–300 °C) to sinter metal particle or to transfer precursor to metal particle. For most popular flexible substrates, such as polyimide (Kapton) and PET (Polyester), the allowed processing temperature is up to 275 °C and 150 °C, respectively. Therefore, the high temperature sintering process will deform the substrate and, as a result, prevent precision alignment for subsequent processes to form high-density circuits. Due to this limitation, it is difficult to fabricate wires by direct ink jet printing of nanoparticles on most of flexible substrates.

We presented here an alternative ink jet approach to form metal circuits. First, the flexible substrate needs to be specially treated to enhance its adhesion, and then the ink jet ink can be free of binder content and achieve high printing quality. In addition, the ink can be water-base catalyst ink to avoid the sintering process needed for nano-particle ink. Under these conditions, the metal circuit can then be fabricated by the transportation of catalyst and metal ion in electroless plating solution at room temperature. The result has been verified by IPC 6013 standard for flexible substrate. This study also developed an image analysis method to validate the reliability of this ink jet printed circuit. It included the step of threshold setting, erosion operation, template calibration, filtering, and edge enhancement.

EXPERIMENTAL

Ink Jet Platform

The ink jet system consists of a specially designed ink jet head for patterning. The head has 300 nozzles and the resolution is 600 dpi; each nozzle discharges the ink drops of 35–85 pico-liter (pL) in volume. The printing system is based on a three-axis X-Y- θ table with micro-step resolution of 0.5 μm up to 4 in/s speed, a set of printing heads, and an

area CCD are fixed on the mechanical support. In operation, the firing distance between the substrate and the print head is adjusted at $500\ \mu\text{m}$ to get better printing quality. A waveform driving procedure is adopted to control the printing stability and quality. For more details, one can refer to Cheng et al.⁴

Measurement Tools

An optical-interferometry three-dimensional (3D) surface profiler was used to measure the thin film profile (SNU Precision Co., Korea). It had a vertical resolution of $0.1\ \text{nm}$, and lateral resolution of $0.5\ \mu\text{m}$. Scanning range can be adjusted from micro to nanometer, depending on the interferometric optics ($2\times-5\times$, Michelson interferometry, $10\times-50\times$, Mirau interferometry).

Fabrication Processes

Before ink jet printing of the catalyst material, a modification of surface property is required to increase the surface adhesion to the catalyst. In this work, we use the PEMs (Polyelectrolyte Monolayer) as our approach for the selective electroless plating of Cu. The key feature of PEMs based on PAH [Poly (allylamine hydrochloride)] and PAA [Poly-(acrylic acid)] is the ability to alter multilayer surface functionalities with a single layer of polyelectrolyte which can selectively bind with a Pd complex. A PAA-dominant surface binds a positively charged Pd complex, while a PAH-dominant surface resists binding. With a negatively charged Pd complex, the PAH-dominant surface binds the catalyst, while a PAA-dominant surface resists binding. Electroless plating was selectively promoted on only the PAA or PAH surface and inhibited on the other with the difference in just one polyelectrolyte layer. PAH/PAA multilayer coated substrates that contain regions of PAA or PAH outermost layer were used for direct plating only to the PAA or PAH surfaces. In this discovery, the PEMs first modified the substrate surface. Then the catalyst was ink jet printed onto the surface for patterning. And, finally, an electroless plating process was used to form the metal wire over the pattern of catalyst. Details about chemical preparation and electroless plating can be found in prior study.⁵

DISCUSSIONS

Circuit Electronic Performance

During the plating process, we controlled the concentration of plating bath at fixed temperature and pH value, and grew the metal thickness by manipulating the plating time. Shiratori⁶ pointed out the surface roughness can influence the thickness of an absorbed monolayer, with thicker layers being formed on multi-layers of high roughness. In this study, the substrate FR-4 has primitive roughness about $2\ \mu\text{m}$ before the SAP layering treatment. Figure 1 showed the curve of plating time versus metal thickness, and it indicated a linear relationship for operations within about $180\ \text{min}$. Over $180\ \text{min}$, the growth rate of the metal film will slow down gradually, and that it exhibits a nonlinear behavior in Fig. 1. The linear average growth rate was estimated at about $16\ \mu\text{m}/150\ \text{min}$, or near $0.1\ \mu\text{m}/\text{min}$ deposition rate. Experimental observation found this non-

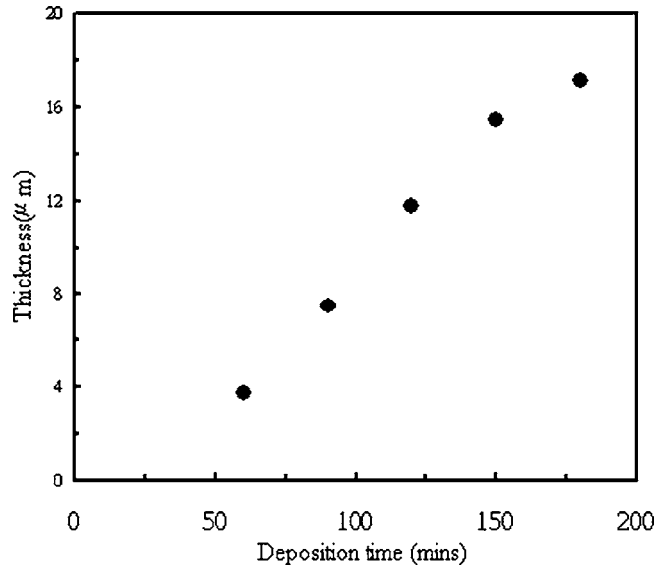


Figure 1. Electroless plating stability curve of deposition time vs metal thickness.

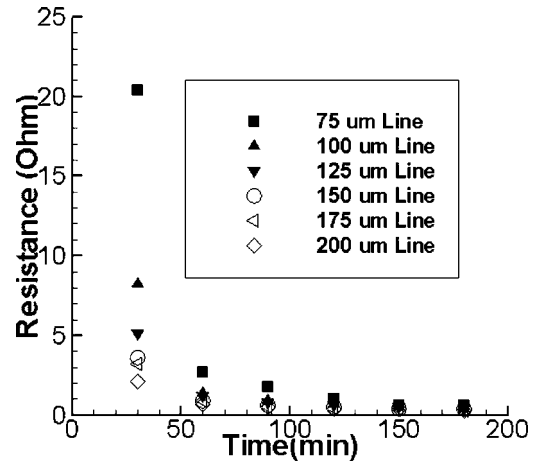


Figure 2. Resistance varies with different line width and electroless plating time.

linear behavior will cause deterioration in the quality of line cross profile, i.e., thinner metal film (linear region) has more flat and near square in cross profile, and it gradually grows toward lateral of line cross profile, due to the slow growth rate of thickness in nonlinear region was comparable with lateral growth rate, and formed a mushroom-type profile.

Figure 2 showed the electrical property data for ink jet printed catalyst lines of various widths after different periods of electroless plating time. The different line width of ink jet printing of catalyst was controlled by the overlap of jetting drops. After the formation of catalyst reminds (Pd), it proceeded the following electroless plating and formed metal (Cu) replaced the Pd. Our observation found the dense catalyst reminds due to overlap will make the thickness difference at initial time period, for example, about $30\ \text{min}$, but it was minor when the plating time over $60\ \text{min}$. It was indicated that the resistance considerably decreases with the increase in plating time, and the resistance varies inversely with the

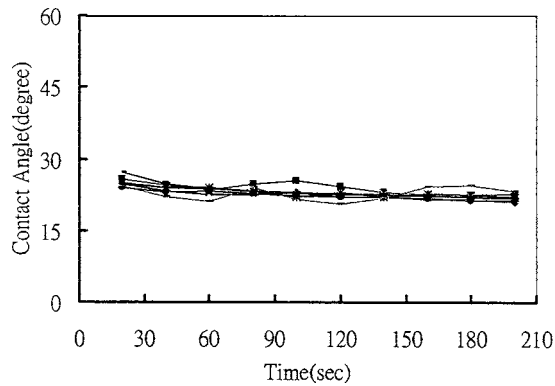


Figure 3. Continuous observation of contact angle between water and FR-4 substrate. Each symbol represents a section on substrate.

line width. For plating time over 60 min, a typical example of the thickness is about $4\ \mu\text{m}$ for any printing of catalyst width, while its resistance is less than $10\ \mu\Omega/10\ \text{cm}$. The best resistance value measured was about $0.304\ \mu\Omega/\text{cm}$ with the metal line width of $250\ \mu\text{m}$ and the line thickness of $17\ \mu\text{m}$. It is about eight times of bulk resistivity of copper ($\rho_{\text{bulk,Cu}} = 1.67\ \mu\Omega/\text{cm}$).

Surface Uniformity

In order to acquire the identical metal line width, surface properties of the polyelectrolyte membranes play an important role. The uniformity of the adsorbed PEMs layers can be monitored by the measurement of contact angle. First, we monitored the variations of contact angle on the substrate surface since the drop has landed. It is noteworthy that the changes in contact angle slow down with time, due to the mass loss by evaporation and slowly wetting of drop on substrate surface. Therefore, it must define a measurement point to clarify the variation of contact angle. In the following measurement in Fig. 4, the measured contact angle was operated at the time of 120 s after the drop had landed on substrate. Figure 4 monitored the variations of contact angle with storage time of substrate has been coated with PEM layers, to verify the environmental effects on the surface property. The result is shown as the curve in Fig. 4. The curve of contact angles measured climbed upwards with storage time, but it reached a plateau at about 70° after several days. It suggests one can fabricate stable PEMs layers, while the numerals of contact angle steadily raised with time until approached to about 70° .

Data Format Transfer

The standard data format used in PCB fabrication is Gerber RS274X. RS274X is a script language to specify the coordinates, angle, width, and other characteristics of the images in the printed circuits. This script language does not describe data in raster format, which is normally used for ink jet printing. Therefore, a conversion step is necessary. The main idea is to convert RS274X to a raster format, for instances, TIFF, JPEG, or BMP. Figures 5(a) and 5(b) are partial original image of a six-layer board in RS274X for a mobile phone, and its converted image in JPEG. There is no visible

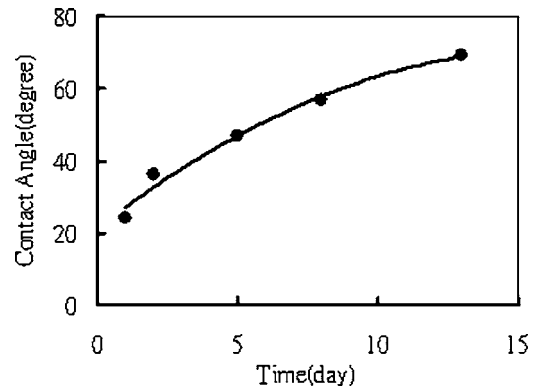


Figure 4. Film stability changes with time. After printing of the catalyst, the substrate was first baked in oven at 40°C for 30 min, and then stored at 40% relative humidity for days.

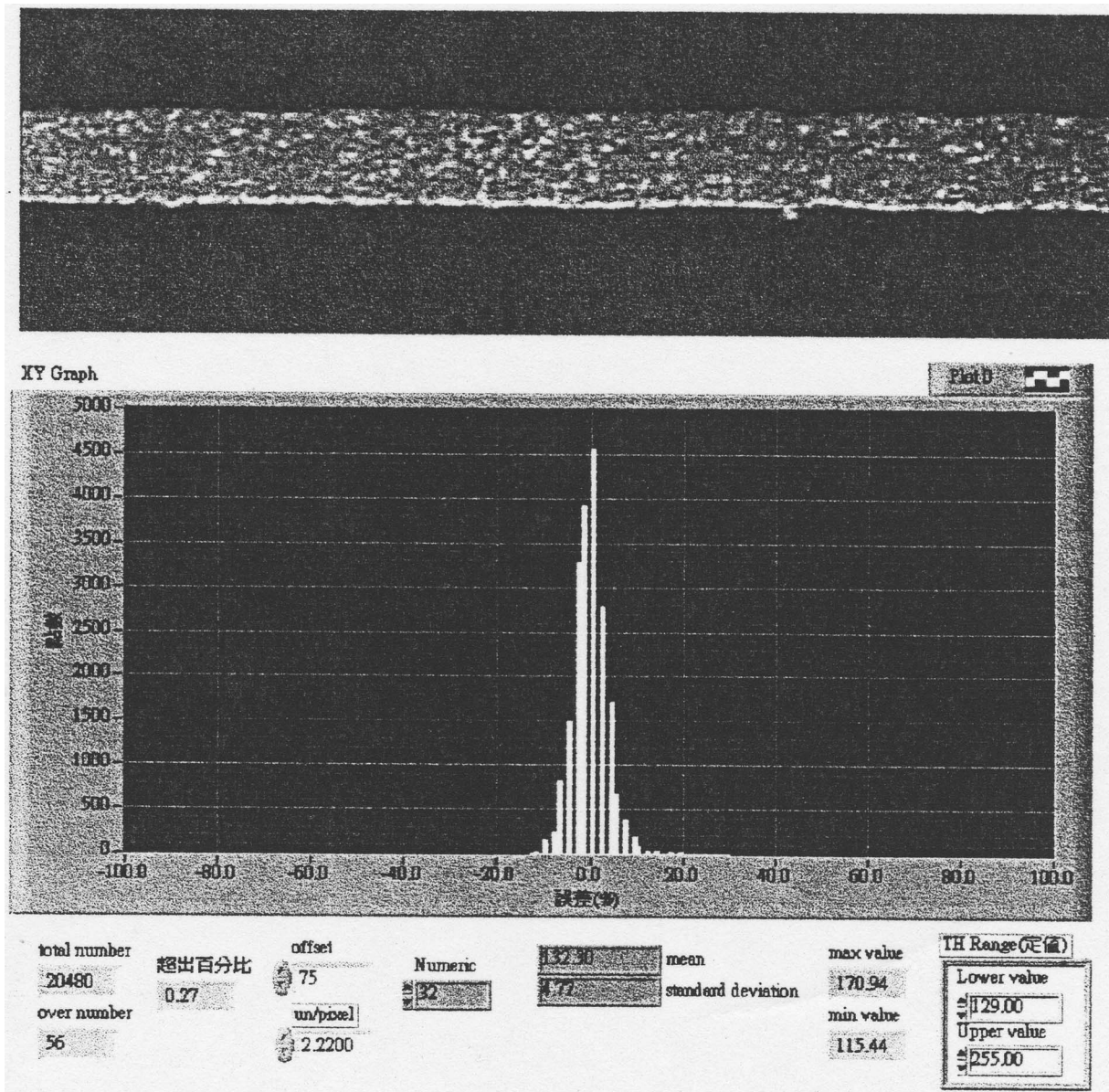
resolution loss between the original and converted images, with conversion resolution up to 4800 dpi.

Image Analysis

When the converted circuit patterns are ink jet printed, it is found that there are deformations introduced during the process. Measurements need to be carried out to preprocess the images to minimize the deformations. First, these deformations introduced by ink jet printing are analyzed to be better understood.

Our study revealed that a majority of the deformations come from abnormal droplet formation, including nozzle cross talks and satellite droplets. Nowadays, ink jet chambers are arranged in a tight array to aim for a high device spatial resolution. They typically share one common liquid supply. As a result, the pressure generated from the firing chamber can affect the menisci at the nozzles of its neighboring chambers, posing "hydraulic crosstalk." Hydraulic crosstalk makes droplet volume control difficult and even causes unexpected droplet ejection when combined with the crosstalk.⁷ Satellite droplet formation is another one of the most troublesome issues. The typical satellite droplet ejection sequence shows that a long tail separates from the primary droplet and breaks into small droplets. Satellite droplets randomly occur alongside the device pattern during ink jet printing, result in line edge blurring and deteriorate the device performance. The crosstalk and satellite drop occurrences will introduce noises to the image background and smear the boundary of the circuit lines. Therefore, it is recommended that the circuit pattern of interest must be carefully filtered and processed before ink jet printed.

Five factors contribute to the overall image quality: Resolution, contrast, depth of field, perspective, and distortion.⁸ In this study, the captured image was processed and analyzed in the steps below. The first is the threshold setting step, mainly to isolate objects of interest in an image. It enables one to select ranges of pixel values to detach the objects under consideration from the background. The second step is to erode object. Erosion eliminates pixels isolated in the background and erodes the counter of particles ac-



(a)



(b)

Figure 5. (a) and (b) Interpretation of Gerber RS274X (a) and JPEG (b).

ording to the template defined by the structuring element. The structuring element defined by a set of matrix data controls the effects of erosion. In this study, a 3×3 matrix with all element values set to one is adopted. The third step is a simple calibration. It transfers pixel coordinates to coordinates of physical dimension through scaling in the X and Y

directions. The fourth step, particle filtering, makes a decision whether to keep or remove particles in an image according to their morphological measurements. It depends on a preset value to isolate the main drops from the satellite drops in the image. The fifth step is the edge-enhancement step. It enhances the edge from background. Through these

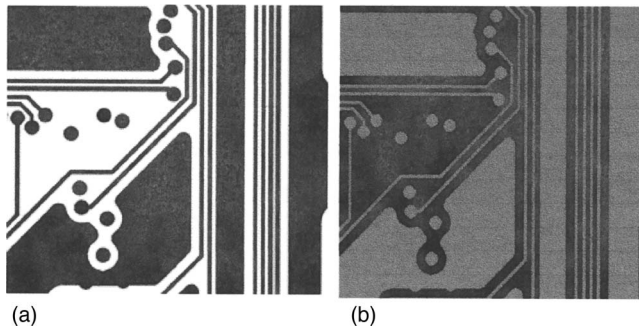


Figure 6. (a) and (b) Analysis of the circuit along with the line direction: (a) Image (b) distribution of the line width variation.

five steps, the line patterns in a circuit image can be enhanced, so that the center and width of the circuit lines can be analyzed.

Figures 6(a) and 6(b) are results from analysis of the circuits fabricated by the aforementioned method. As shown in Fig. 6(a), the captured image has an average line width of $135\ \mu\text{m}$ and a standard deviation of $3.5\ \mu\text{m}$. Figure 6(b) presented the variation of distribution along horizontal direction. It indicated a maximum $\pm 15\%$ blurring rate.

Circuit Reliability

IPC 6013⁹ covers mechanical, electrical qualification as well as performance requirements for printed wiring on flexible substrates. In this standard, the printed wiring on flexible substrates may be single-sided, double-sided, multilayer, or rigid-flex multilayer. All of these constructions may or may not include stiffeners, plated-through holes, or blind/buried via. In this study, the ink jet printed circuit had been verified following the testing standard of IPC 6013, as shown in Table I. To verify the adhesion capability, the 3M tape (3M, No. 600, 1/2 in width, 2 in length) was attached to the substrate and then peeled at vertical direction. No trifles were left on the tape. The outcome showed excellent adhesion between the circuit and the flexible substrate. The significant improvement of the adhesive properties was primarily because of the modification of the PEMs Layer to the substrate. Claesson¹⁰ mentioned that the adhesion between one

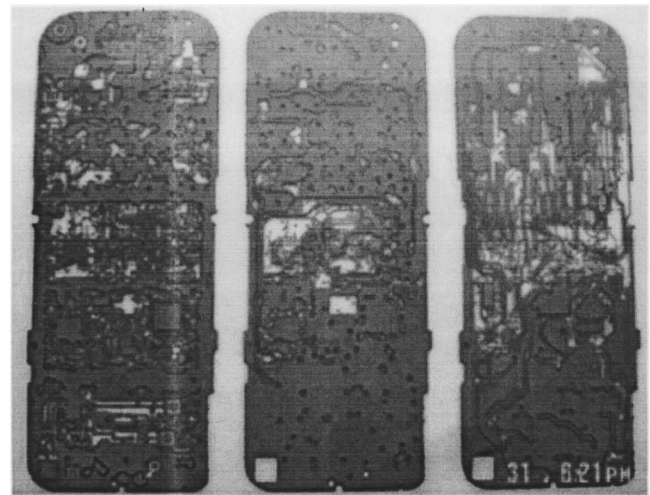


Figure 7. High-density circuit board for mobile phone fabricated by ink jet printing of catalyst and electroless plating.

polyelectrolyte-coated surface and one bare surface was initially stronger than that between the two polyelectrolyte-coated surfaces. However, due to the material transfer between the two surfaces, the adhesion decreased significantly with the number of times that the surfaces were driven into contact. For the polyelectrolytes of the lowest charge density, the results suggest that the entanglement effects contributed to the adhesive interaction.

An important requirement of the circuit quality is the resistance to thermal cycles, especially during the soldering procedure. In the standard procedure, the sample was first baked at $120\text{--}150\ ^\circ\text{C}$ for 6 h to drive the moisture away, and then the sample was moved to room temperature environment to cool down. The circuit went under a thermal stress test at $288\ ^\circ\text{C} \pm 5\ ^\circ\text{C}$ for six times and was immersed in $260\ ^\circ\text{C} \pm 5\ ^\circ\text{C}$ hot oil for three times. The circuit sample was able to endure both testing conditions. The details can be found in Table I.

Figure 7 shows the high-density circuit board fabricated. In Fig. 7, the image pattern is mostly composed by circle pads, square pads, and narrow metal wires. Where the cop-

Table I. Environmental testing results followed the IPC 6013 standard.

Testing Item	Results	Testing Conditions
Peeling test	Pass	3 M tape
Thermal stress	Pass.	$288\ ^\circ\text{C} \pm 5\ ^\circ\text{C}$, 6 times
Hot oil test	Pass	$260\ ^\circ\text{C} \pm 5\ ^\circ\text{C}$, 3 times
Soldering test	Pass	Soldering tin on circuit within 10 s
Dielectric Withstanding Voltage	Pass	Class 3 100 Vdc, 30 s
Peeling stress	Excellent adhesion which cannot peel the metal line to be tested. Stress should $>245\ \text{MPa}$ for $50\text{--}100\ \mu\text{m}$ thickness, and elongation rate large than 12% at room temperature.	

per metal line was formed by ink jet printing catalyst, and then electroless plating over the SAP treated FR4 substrate. The line width is less than 100 μm and the thickness is near 12 μm . Overall fabrication time was only about three hours; most of the time was spent on the film thickness required, for example, 2 h for about 12 μm . Key factors for controlling the film thickness are the plating bath concentration, bath temperature, pH stability, additives, and the plating time. In our work, we kept all the factors constant except the plating time.

CONCLUSIONS

This paper developed a method for fabricating circuits on flexible substrates by combining self-assembled polyelectrolytes, ink jet printing of catalyst, and electroless plating of metals. The study found that this novel procedure yielded excellent selection capability and adhesion on various substrates. To our knowledge, this is the first time such technology has been implemented successfully for electronic circuits conforming to the IPC standard. Compared with the photo process like laser chemical vapor deposition (LCVD) and screen printing (SP) technology,^{11–16} this novel fabrication has the benefits of: (1) Room temperature operation, for most of LCVD, their operation temperature generally at the range of 300 °C–400 °C and not suitable flexible substrate; (2) low copper resistivity, the copper process was difficult for LCVD, and the best published data has reached about 25 $\rho_{\text{Cu,Bulk}}$ (copper resistivity in bulk), by this study, less than 8 $\rho_{\text{Cu,Bulk}}$ is feasible; (3) fine line width, typical line width for SP was limited above 75 μm and hard to improve in future, ink jet printing has the competition at the range of 10–75 μm .

Considering the ink jet characteristics, an image process method including the step of threshold setting, erosion op-

eration, template calibration, filtering, and edge-enhancement was also developed to analyze the circuit quality. Further study will focus on methods to fabricate finer lines and analysis of the effects of the ink jet printing algorithm on sub-patterns of the circuit, such as circle, wire connections, vertical lines and angled lines.

REFERENCES

- ¹K. F. Teng and R. W. Vest, *IEEE Electron Device Lett.* **9**, 591 (1988).
- ²T. Oguchi, K. Suganami, T. Nanke, and T. Kobayashi, *Proc. IS&T's NIP 19* (IS&T, Springfield, VA, 2003) pp. 656–659.
- ³C. Curtis, T. Rivkin, A. Miedaner, J. Alleman, J. Perkins, L. Smith, and D. Ginley, *National Renewable Energy Laboratory Report* (2001).
- ⁴K. Cheng et al., *Proc. IS&T's NIP 19* (IS&T, Springfield, VA, 2003) pp. 309–313.
- ⁵K. Cheng, M.-H. Yang, W. W. W. Chiu, C.-Y. Huang, J. Chang, and T.-F. Ying, "Ink jet printing, self-assembled polyelectrolytes, and electroless plating: Low cost fabrication of circuits on flexible substrate at room temperature", *Macromol. Rapid Commun.* (to be published).
- ⁶S. S. Shiratori and M. F. Rubner, *Macromolecules* **31**, 4309 (1998).
- ⁷F.-G. Tseng, C.-J. Kim, and C.-M. Ho, *J. Microelectromech. Syst.* **11**(5), 427–436 (2002).
- ⁸R. C. Gonzalez and R. E. Woods, *Digital Image Processing* (Addison-Wesley, Reading, MA, 1993).
- ⁹"IPC 6011 Generic Performance Specification for Printed Board", Edited by IPC Association Connecting Electronics Industries, 1996, www.ipc.org.
- ¹⁰P. M. Claesson, A. Dedinaite, and O. J. Rojas, *Adv. Colloid Interface Sci.* **104**, 53–74 (2003).
- ¹¹M. Meunier, R. Izquierdo, M. Tabbal, S. Evoy, P. Desjardins, N. Elyaagoubi, M. Suys, and E. Sacher, *Mater. Sci. Eng., B* **45**, 200–207 (1997).
- ¹²M. Wehner, F. Legewie, B. Theisen, and E. Beyer, *Appl. Surf. Sci.* **106**, 406–411 (1996).
- ¹³K. Kordás, L. Nánai, G. Galbács, A. Uusimäki, and S. Leppävuori, *Appl. Surf. Sci.* **158**, 127–133 (2000).
- ¹⁴Y. B. Hahn, S. J. Pearton, H. Cho, and K. P. Lee, *Mater. Sci. Eng., B* **79**, 20–26 (2001).
- ¹⁵W. Pfleging, A. Vörckel, H. Duddek, D. A. Wesner, and E. W. Kreutz, *Appl. Surf. Sci.* **109/110**, 194–200 (1997).
- ¹⁶D.-Q. Yang and E. Sacher, *Surf. Sci.* **516**, 43–55 (2002).